Bioorganic & Medicinal Chemistry 18 (2010) 6258–6264

Contents lists available at ScienceDirect

Bioorganic & Medicinal Chemistry

journal homepage: www.elsevier.com/locate/bmc

Xanthones with neuraminidase inhibitory activity from the seedcases of *Garcinia mangostana*

Hyung Won Ryu [a], Marcus J. Curtis-Long [c], Sunin Jung [a], Young Min Jin [a], Jung Keun Cho [a], Young Bae Ryu [b], Woo Song Lee [b,*], Ki Hun Park [a,*]

[a] Division of Applied Life Science (BK21 Program), EB-NCRC, Institute of Agriculture & Life Science, Graduate School of Gyeongsang National University, Jinju 660-701, Republic of Korea
[b] Eco-Friendly Biomaterial Research Center, KRIBB, Jeongeup 580-185, Republic of Korea
[c] 12 New Road, Nafferton, East Yorkshire YO25 4JP, UK

ARTICLE INFO

Article history:
Received 24 May 2010
Revised 13 July 2010
Accepted 14 July 2010
Available online 19 July 2010

Keywords:
Garcinia mangostana
Xanthone
Neuraminidase
Time-dependent

ABSTRACT

This study was designed to gain deeper insights into the molecular properties of natural xanthones as neuraminidase inhibitors. A series of xanthones **1**–**12** was isolated from the seedcases of *Garcinia mangostana* and evaluated for bacteria neuraminidase inhibitory activity. Compounds **11** and **12** emerged to be new xanthones (mangostenone F, mangostenone G) which we fully spectroscopically characterized. The IC_{50} values of compounds **1**–**12** were determined to range between 0.27–65.7 μM. The most potent neuraminidase inhibitor **10** which has an IC_{50} of 270 nM features a 5,8-diol moiety on the B ring. Interestingly, structure–activity studies reveal that these xanthones show different kinetic inhibition mechanisms depending upon the arrangement of hydroxyl groups in the B ring. Compound **6** possessing a 6,7-diol motif on the B-ring operated under the enzyme isomerization model ($k_5 = 0.1144\ \mu M^{-1}\ s^{-1}$, $k_6 = 0.001105\ s^{-1}$, and $K_i^{app} = 7.41\ \mu M$), whereas compound **10** possessing a 5,8-diol unit displayed simple reversible slow-binding inhibition ($k_3 = 0.02294\ \mu M^{-1}\ s^{-1}$, $k_4 = 0.001025\ s^{-1}$, and $K_i^{app} = 0.04468\ \mu M$).
© 2010 Elsevier Ltd. All rights reserved.

1. Introduction

The neuraminidase (EC 3. 2. 1. 18) family is a group of exo-acting enzymes that hydrolyze terminal sialic acids from a variety of glycoproteins.[1,2] This enzyme specifically cleaves *N*-acetylneuraminic acid (Neu5Ac) from cell-surface glycoproteins when sialic acid is joined to galactose via an α2 → 3 or α2 → 6 linkage.[3–5] Sialic acids are primarily found at terminal positions of numerous glycoconjugates, and are important in a varied array of cell–cell interactions and cell–molecule recognition processes.[6,7] Neuraminidase has a well known role in infectivity of the influenza virus, however the precise role that bacterial neuraminidase plays in pathogenesis has not been clearly established.[8] However both protective and aggressive roles for neuraminidase have been described. Recent studies have shown that several bacterial pathogens can attach sialic acid residues (sialylate) to their outer surfaces enabling them to evade the host immune system.[9] As mucosal surfaces are heavily sialylated, neuraminidases are thought to modify epithelial cells by exposing potential bacterial receptors.[10] Bacteria can also utilize sialic acid as both a carbon and nitrogen source by scavenging it from the surrounding environment.[11,12] Many pathogens, including *Streptococcus pneumoniae*, *Peudomonas aeruginosa*, and *Clostridium perfringens*, express neuraminidase that can cleave sialic acid from glycoconjugates. For example, *C. perfringens* secrete multimodular sialidases, which remove terminal sialic acid residues from glycans. These sialidases can act as virulence factors.[13] This process has important implications for human infection such as the potentiation of α-toxin and the cause of hemolysis during blood transduction.[14] Neuraminidase is also believed to pay critical roles in the interplay of bacteria with their human hosts both in symbiotic relationships and pathogenic ones.[15] For instance, Soong et al. reported that bacterial neuraminidase facilitates mucosal infection by participating in biofilm production.[8] Thus development of inhibitors of neuraminidase may provide a new weapon for the treatment of bacterial pathogenic diseases that arises from hydrolysis of sialic acid.

Recently, we disclosed the first report that a natural xanthone analog exhibited inhibitory activity against neuraminidase.[16] This encouraged us to investigate the seedcases of *Garcinia mangostana* (Mangosteen) since xanthones are its principal class of secondary metabolite.[17] In this study, we isolated 12 xanthones including two new xanthones from Mangosteen that are moderate to excellent inhibitors of neuraminidase. The isolated xanthones provide a

Abbreviations: I, intensity at ex: 365 nm, em: 450 nm; IC_{50}, the inhibitor concentration leading to 50% activity loss; K_i, inhibition constant; K_i^{app}, apparent K_i; k_{obs}, apparent first-order rate constant for the transition from v_i to v_s; v_i, initial velocity; v_s, steady-state velocity.

* Corresponding authors. Tel.: +82 63 570 5170 (W.S.L.); tel.: +82 55 751 5472; fax: +82 55 757 0178 (K.H.P.).
E-mail addresses: wslee@kribb.re.kr (W.S. Lee), khpark@gnu.ac.kr (K.H. Park).

0968-0896/$ - see front matter © 2010 Elsevier Ltd. All rights reserved.
doi:10.1016/j.bmc.2010.07.033

sufficient range of chemotypes to allow numerous insights into the SAR. Interestingly, xanthone analogs showed either enzyme isomerization or simple reversible slow-binding inhibition depending on the positions of hydroxyl group in B ring.

2. Results and discussion

2.1. Isolation and identification of xanthone analogs

Repeated chromatography of the chloroform extract of the seedcases of Mangosteen yielded 12 xanthones (Fig. 1). The spectroscopic data of compounds (**1**–**10**) agree with those previously published for β-mangostin (**1**), 9-hydroxycalabaxanthone (**2**), mangostanol (**3**), α-mangostin (**4**), garcinone D (**5**), γ-mangostin (**6**), cudraxanthone (**7**), 8-deoxygartanin (**8**), gartanin (**9**), and smeathxanthone A (**10**).[18–26]

Compounds **11** and **12** were identified as new compounds that were named as mangostenone F and mangostenone G, respectively. Compound **11** was obtained as a yellow solid having the molecular formula $C_{24}H_{24}O_6$ and 13 degrees of unsaturation established by HREIMS (*m/z* 408.1571 $[M]^+$). ^1H and ^{13}C NMR data in conjunction with DEPT experiments enabled carbons corresponding to the carbonyl and eight C–C double bonds to be identified, and thus accounted for nine of 13 degrees of unsaturation. The extra four degrees of unsaturation were ascribed to a tetra cyclic ring system (including a xanthone ring). The presence of a 3,3-dimethylallyl group was deduced from successive connectively from H-16 (δ_H 3.98) to H-20 (δ_H 1.52) in the COSY spectrum. HMBC correlation of the peak at δ_H 3.98 (H-16) with C-8 (δ_C 131.8) unveiled the location of the 3,3-methylallyl moiety (Fig. 2). The presence of a 2″-isopropenyldihydrofurano group was confirmed from successive connectively between methylene protons H-11a/b (δ_H 2.75, 2.94) to vinylic protons H-14a/b (δ_H 4.62, 4.82) that have also connectively with H-15 in the COSY spectrum. The location of the 2″-isopropenyldihydrofurano group was proven by HMBC correlation between H-11 and C-1 (δ_C 162.6), C-2 (δ_C 109.4), and C-3 (δ_C 165.1). The location of the methoxy group was easily confirmed by HMBC correlation between CH_3O (δ_H 3.66) and C-7 (δ_C 145.0). Thus, compound **11** was identified as 4,8-dihydroxy-7-methoxy-6-(3-methylbut-2-enyl)-2-(prop-1-en-2-yl)-2,3-dihydrofuro[3,2-*b*]-xanthen-5-one, and called mangostenone F (Fig. 2).

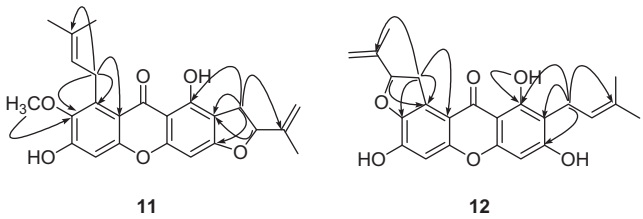

Figure 2. Selected HMBC correlations for new compounds **11** and **12**.

Compound **12** was obtained as a yellow solid having the molecular formula $C_{23}H_{22}O_6$ and 13 degrees of unsaturation by HREIMS (*m/z* 394.1419 $[M]^+$) and DEPT experiments. The 3,3-dimethylallyl and 2″-isopropenyldihydrofurano groups were deduced by interpretation of NMR spectra which have very similar patterns to compound **11**. The position of the 3,3-dimethyl moiety on the B ring was determined by HMBC correlation between H-11 (δ_H 3.21) to C-1 (δ_C 162.0), C-2 (δ_C 111.3), and C-3 (δ_C 163.3). The position of C-1 was clearly confirmed by the presence of a hydrogen bonded hydroxyl group (δ_H 13.6) and a strong HMBC correlation between O*H* (δ_H 13.6) and C-1 (δ_C 162.0). The HMBC correlations of H-16a/b (δ_H 2.93, 4.11) to C-7 (δ_C 143.3), C-8 (δ_C 128.1), and C-8a (δ_C 112.4) were also observed. Thus, compound **12** was identified as 4,8,10-trihydroxy-9-(3-methylbut-2-enyl)-2-(prop-1-en-2-yl)-1,2-dihydrofuro[3,2-*a*]xanthen-11-one called mangostenone G (Fig. 2).

2.2. Effects of isolated xanthones on the activity of neuraminidase

Among the xanthones we isolated, the array of hydroxyl/alkoxy groups in the A ring is relatively fixed in a 1,3 arrangement. However the regioisomeric distribution and number of oxygen atoms around the B ring (6,7-dihydroxy, 5,8-dihydroxy, or 5-hydroxy substitution) varies quite considerably, and has allowed us to draw a number of insights into the SAR of these compounds. These compounds were evaluated for their inhibitory effects toward neuraminidase activity. For this assay, we used neuraminidase from *C. perfringens* which belongs to the glycosyl hydrolase 33 family and hydrolyses α2 → 3, α2 → 6, and α2 → 8 glycosidic linkages of

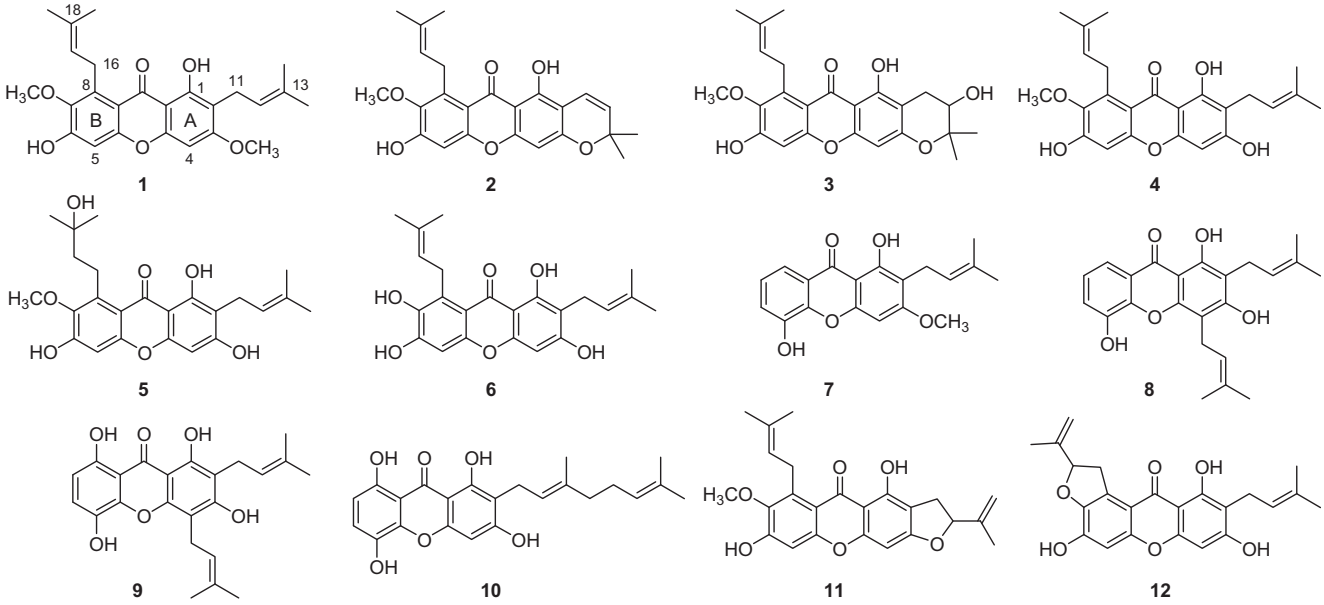

Figure 1. Chemical structures of isolated compounds **1**–**12** from the *Garcinia mangostana*.

terminal sialic acid residues. The tested compounds exhibited significant dose-dependent inhibition with IC_{50}s in the range 0.27–65.7 μM (Table 1).

Our data show some interesting facets of the SAR. It appears that better inhibition is observed when there are two free hydroxyl groups in the B ring. This can be seen by comparing compound **6** with methyled analog **1** and **4**. The number free hydroxyl group influenced the potency of inhibition: **6** (IC_{50} = 2.2 μM) > monomethyl analog **4** (IC_{50} = 12.2 μM) > dimethyl analog **1** (IC_{50} = 60.7 μM). In comparing of prenyl group and prenyl hydrate, prenyl hydrate (**5**, IC_{50} = 5.7 μM) was more effective than prenyl group (**4**, IC_{50} = 12.2 μM) because it presumably relates with hydrogen bonding site. A similar requirement is also found in the A ring when the C(3)OH is capped with a methyl group and to a lesser extent a hemiterpene fragment. Thus **1** is much less potent than **4** whereas as **2** is only slightly less potent than **4**. The latter presumably implies that conformation/orientation of the alkyl appendage is important in this position. In 5,8-dihydroxy derivatives, 8-position hydroxyl group plays a critical role for inhibition because dramatic difference of IC_{50} was observed between compound **9** (IC_{50} = 2.9 μM) and 8-deoxy compound **8** (IC_{50} = 29.2 μM). Alkyl appendage was also a critical factor for inhibition. For example, geranylated xanthone (**10**, IC_{50} = 0.27 μM) is 10 times effective than prenyl xanthone (**9**, IC_{50} = 2.9 μM).

All inhibitors manifested a similar relationship between enzyme activity and concentration. Raising the concentrations of the inhibitors drastically lowered residual enzyme activity. The relevant data for compound **6** is illustrated in Figure 3B as an example. Plots of residual enzyme activity versus enzyme concentration at different concentrations of compound **6** gave a family of straight lines with a common *y*-axis intercept, indicating that **6** is a reversible inhibitor. Augmenting the concentration of compound **6** resulted in a reduction of the slopes of the lines.

Subsequently, the kinetic behavior of hydrolysis of 4-methylumbelliferyl-α-D-*N*-acetylneuraminic acid, catalyzed by neuraminidase at different concentrations of all isolated compounds (**1**–**12**) was studied. All compounds showed competitive inhibition behavior (Table 1). The inhibition profiles of 6,7-diol derivatives **2** and **6** and also 5,8-diols **9** and **10** (Fig. 3). As depicted in Figure 3C–F, the inhibition kinetics analyzed by Lineweaver–Burk plots show that compounds **2** [(k_i = 5.9 μM, C], **6** [(k_i = 0.8 μM), D], **9** [(k_i = 3.6 μM), E], and **10** [(k_i = 0.15 μM), F] are competitive inhibitors because increasing concentration resulted in a family of lines with a common intercept on the *y*-axis but with different gradients.

Table 1
Inhibitory effects of compounds (**1**–**12**) on neuraminidase activities

Compound	Neuraminidase	
	IC_{50}[a] (μM)	Kinetic mode (K_i, μM)[b]
1	60.7 ± 1.5	Competitive (24.9)
2	20.1 ± 1.1	Competitive (5.9)
3	21.5 ± 0.4	Competitive (6.5)
4	12.2 ± 1.2	Competitive (5.8)
5	5.7 ± 0.8	Competitive (3.3)
6	2.2 ± 0.4	Competitive (0.8)
7	65.7 ± 2.1	Competitive (35.2)
8	29.2 ± 0.7	Competitive (15.5)
9	2.9 ± 0.3	Competitive (3.6)
10	0.27 ± 0.05	Competitive (0.15)
11	24.8 ± 0.6	Competitive (7.6)
12	14.6 ± 0.8	Competitive (6.8)
Quercetin	9.8 ± 0.2	NT[c]

[a] All compounds were examined in a set of experiments repeated three times; IC_{50} values of compounds represent the concentration that caused 50% enzyme activity loss.
[b] Values of inhibition constant.
[c] Not tested.

Most strikingly, isolated inhibitors showed a typical progress curve of time-dependent inhibition behavior (vide infra).

2.3. Time-dependent inhibitory effects of xanthones on neuraminidase

To further investigate the inhibition mechanism, the time dependence of the inhibition of the hydrolysis of 4-methylumbelliferyl-α-D-*N*-acetylneuraminic acid by these inhibitors was subsequently probed. This was achieved by measuring initial velocities of substrate hydrolysis as a function of preincubation time of the enzyme with the potent inhibitors 6,7-dihydroxy xanthone **6** and 5,8-dihydroxy xanthones (**9** and **10**) representatively. The enzyme was preincubated with inhibitor for a duration of between 0 and 120 min in 30-min intervals, and the velocity of the reaction was measured as a function of incubation time and analyzed according to Eq. 3. The enzyme was found to lose no more than 20% of activity across the whole assay (control). At fixed inhibitor concentrations, the residual velocity decayed exponentially with preincubation time. Such behavior is typical of a slow-binding inhibitor as shown in Figure 4A. In Figure 4B the data were fitted to Eq. 4 and showed a hyperbolic dependence (R^2 = 1) on the concentration of the inhibitor **6**, so that the inhibition by **6** is believed to followed mechanism A in Scheme 1. The *y* intercept of the curve provides an estimate of the rate constant k_6, while the maximum value of k_{obs} expected at infinite inhibitor concentration. Eq. 4 could also allow the kinetic parameters k_5, k_6 and K_i^{app} to be calculated. These are shown in Table 2. The results indicated that 6,7-dihydroxy xanthone **6** inhibits neuraminidase by rapid formation of an enzyme substrate complex (Enz-I) which slowly isomerizes to form a modified enzyme complex (Enz^*·I).

On the other hand, as illustrated in Figure 4C, xanthones (**9** and **10**) were found to display a linear dependence of k_{obs} versus inhibitor concentration, consistent with the single-step mechanism depicted in Scheme 1B. The dependence of k_{obs} on neuraminidase can be fit to Eq. 3, while k_3, k_4, and K_i^{app} can be fit Eqs. 5 and 6. From the result of the fit, kinetic parameters of both compounds are described in Table 2. From Eq. 3, a plot of k_{obs} as function of [I] produced a straight line with slope equal to k_4/K_i^{app} and *y* intercept equal to k_4. This is a characteristic feature of 5,8-dihydroxy xanthones (**9** and **10**), which indicates simple reversible slow-binding mode.

In sum, the structure–activity studies reveal that xanthones from *G. mangostana* are potent competitive inhibitors with a chemospecific inhibition mechanism. Compound **6** possessing 6,7-diol motif on B-ring operated under the enzyme isomerization model, whereas compound **10** possessing 5,8-diol motif displayed simple reversible slow-binding inhibition.

3. Conclusion

We were thus able to isolate 12 xanthones which exhibited a range of functionality in both the A ring and the B ring. We progressed to conduct SAR investigations. We were able to uncover that the presence of two free hydroxyl groups in the A and B rings was optimal for activity: blocking one of these groups with a methyl or a hemiterpene unit reduced activity. Removing the OH group all together was also detrimental. However, the penalty paid in terms of potency by blocking an OH group with an alkyl group was similar for bulky and methyl functions. We progressed to investigate the kinetic mode of these inhibitors. They all emerged to be competitive inhibitors by Lineweaver–Burk analysis. However, it transpired after detailed kinetic analysis that the differing array of hydroxyl groups on the B ring led to different inhibition mechanisms. Compound **6** bearing a 6,7-diol unit on the B ring was a time-dependent inhibitor which caused enzyme isomerization. On the other hand, the 5,8-diol regioisomer **10**

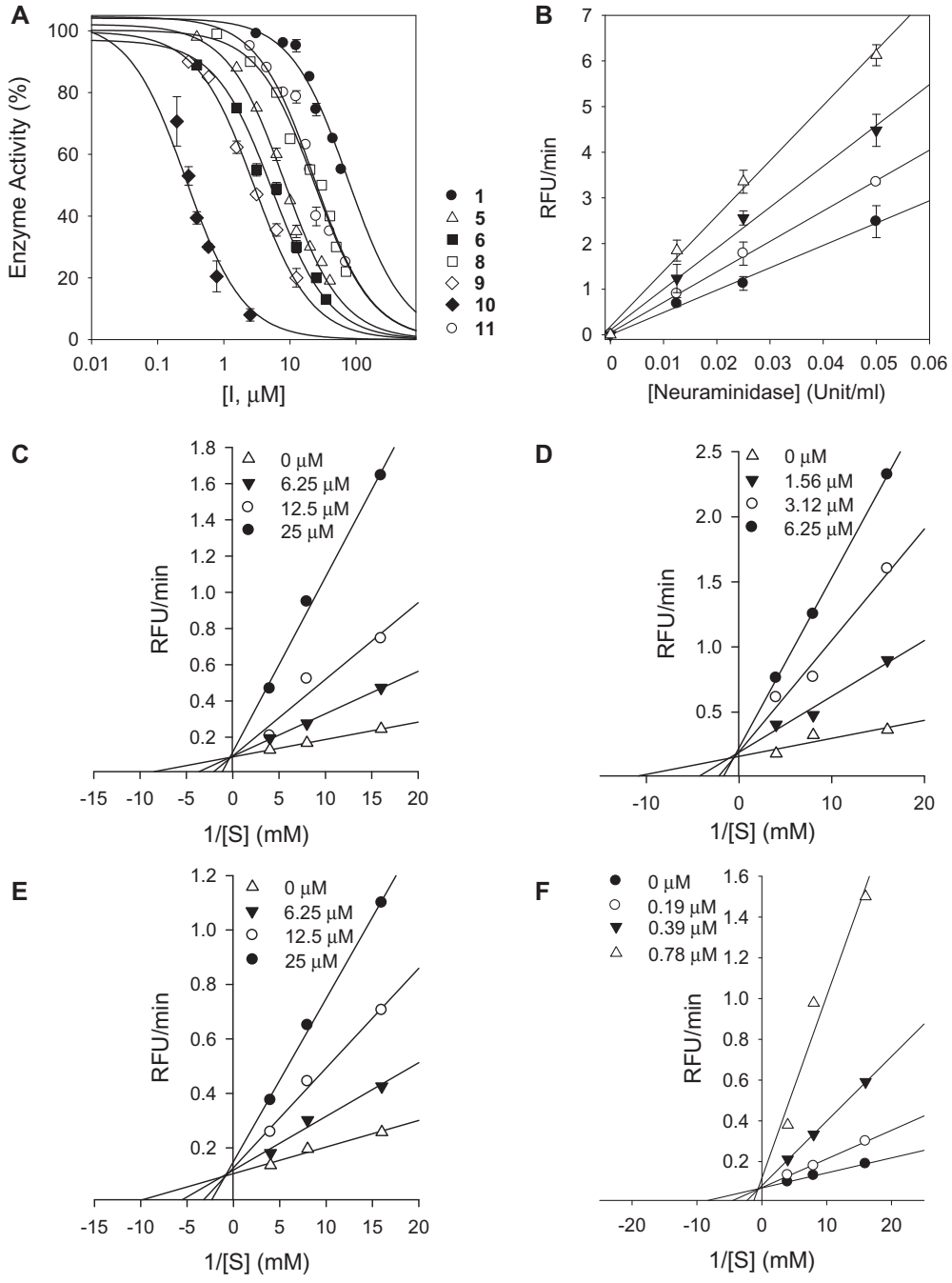

Figure 3. (A) Effects of compounds on the activity of neuraminidase for hydrolysis of 4-methylumbelliferyl-α-D-*N*-acetylneuraminic acid. (Compound **1**, ●; compound **5**, △; compound **6**, ■; compound **8**, □; compound **9**, ◇; compound **10**, ♦; compound **11**, ○, respectively.) (B) The hydrolytic activity of neuraminidase as function of concentration of compound **6** (0, △; 1.5 μM, ▼; 3.1 μM, ○; 6.2 μM, ●, respectively). (C–F) Lineweaver–Burk plot for inhibition of the neuraminidase catalyzed hydrolysis of substrate by compounds (**2**, **6**, **9**, and **10**).

displayed simple time dependent reversible kinetics. We believe that these compounds are interesting lead compounds for the future as neuraminidase inhibition is a hugely important area of research. Our relatively detailed SAR can also help to guide/streamline further research efforts with our kinetic analysis allowing a prediction of the mode of inhibition.

4. Materials and methods

4.1. General apparatus and chemicals

All the reagent grade chemicals were purchased from Sigma Chemical Co. (St. Louis, MO, USA). Chromatographic separations were carried out by Thin-layer Chromatography (TLC) (E. Merck Co., Darmastdt, Germany), using commercially available glass plates pre-coated with silica gel and visualized under UV at 254 and 366 nm sprayed with H_2SO_4 staining reagent. Silica gel (230–400 mesh, Merck), RP-18 (ODS-A, 12 nm, S-150 mM, YMC), and Sephadex LH-20 (Amersham Biosciences) were used for column chromatography. Melting points were measured on a Thomas Scientific Capillary Melting Point Apparatus and are uncorrected. UV spectra were measured on a Beckman DU650 spectrophotometer, Infrared (IR) spectra were recorded on a Bruker IFS66 infrared Fourier transform spectrophotometer (on KBr disks). ^1H and ^{13}C NMR along with 2D NMR data were obtained on a Bruker AM 500 (^1H NMR at 500 MHz, ^{13}C NMR at 125 MHz) spectrometer in $CDCl_3$,

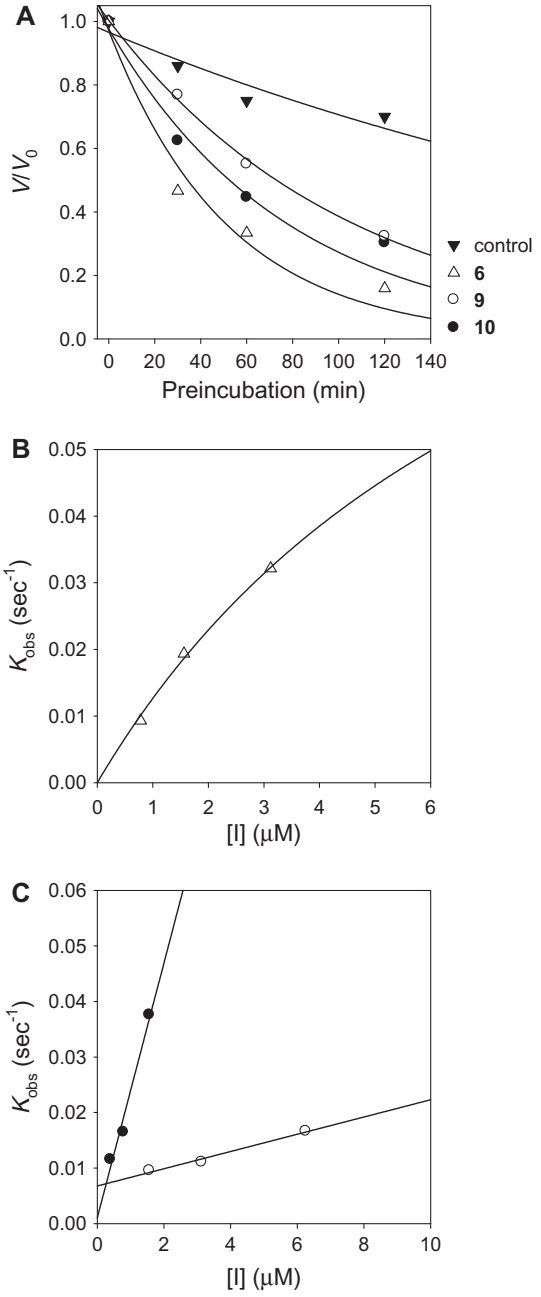

Figure 4. (A) Inhibition as a function of preincubation time for the most active compounds (**6**, 1.56 μM; **9**, 1.56 μM; and **10**, 0.39 μM) at IC_{50}. (B) Plot of k_{obs} as a function of inhibitor **6** concentration for a slow-binding inhibitor fitted by Eq. 4 (**6**, △). (C) Plot of k_{obs} as a function of inhibitors (**9** and **10**) concentration for a slow-binding inhibitor fitted by Eq. 5 (○, **9**; ●, **10**).

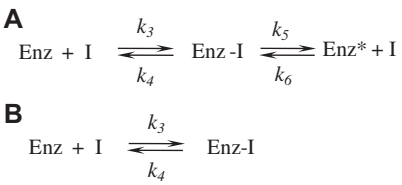

Scheme 1. (A) Enzyme isomerization, (B) Simple (capital) reversible slow-binding inhibition.

Table 2
Kinetic parameters for time-dependent inhibition of neuraminidase by compounds **6**, **9**, and **10**

Compound	K_i^{app} (μM)	k_3 ($\mu M^{-1} s^{-1}$)	k_4 (s^{-1})	k_5 (s^{-1})	k_6 (s^{-1})
6	7.410	—	—	0.1144	0.001105
9	0.43666	0.01552	0.006777	—	—
10	0.04468	0.02294	0.001025	—	—

acetone-d_6, and DMSO-d_6. EIMS and HREIMS data were collected on Jeol JMS-700 spectrometer.

4.2. Isolation of neuraminidase inhibitors from *G. mangostana* pericarp

Garcinia mangostana pericarp from Vietnam was purchased from local fruit stores and stored frozen in a −20 °C freezer for further use. The seedcases of *G. mangostana* (2.3 kg) were air-dried, pulverized, and extracted with chloroform for 3 days at room temperature. The combined extract was evaporated to dryness under reduced pressure at a temperature below 35 °C to afford $CHCl_3$-soluble extracts (65.7 g). The $CHCl_3$ extract was subjected to column chromatography on silica gel (10 × 30 cm, 230–400 mesh, 700 g) using $CHCl_3$/acetone [100:1 (1.5 L), 50:1 (1.5 L), 30:1 (1.5 L), 20:1 (1.5 L), 10:1 (3 L), 6:1 (2.5 L), 4:1 (2 L), 2:1 (2 L), 1:1 (1 L) and only acetone (2 L)] mixtures to give fractions F1–F7. Fraction F1 (7.9 g) was fractionated by silica gel flash CC employing a gradient of hexane to EtOAc resulting in nine subfractions (F1.1–F1.9). Subfractions F1.6–F1.8, enriched with compounds **1** and **2**, were combined (870 mg) and further purified by silica gel flash CC to yield compounds **1** (52 mg) and **2** (25 mg). Fraction F2 (24.1 g) was fractionated by silica gel flash CC employing a gradient of hexane to EtOAc resulting in 32 subfractions (F2.1–F2.32). Subfractions F2.12–F2.23, enriched with compounds **11, 4, 7**, and **8**, were combined (4.3 g) and further purified by silica gel flash CC to yield compounds **11** (48 mg) and **8** (65 mg), and a mixture of compounds **4** and **7**. Further purification of the mixture of **4** and **7** on Sephadex LH-20 (Pharmacia Biotech AB, Uppsala, Sweden) with CH_3OH as eluant yielded compounds **4** (453 mg) and **7** (118 mg). Fraction F3 (18.0 g) was subjected to flash CC employing a gradient of $CHCl_3$ to acetone giving 12 Subfractions (F2.1–F2.12). Subfraction F2.3 and F2.3, enriched with compounds **12**, and **3**, were combined (1.2 g) and further purified by reversed-phase CC (ODS-A, 12 nm, S-150 μM) eluting with CH_3OH/H_2O (4:1) to afford compounds **12** (8 mg), and **3** (18 mg). Fraction F4 (8.5 g) was subjected to flash CC employing a gradient of $CHCl_3$ to acetone giving 20 Subfractions (F4.1–F4.20). Subfraction F4.3 and F4.4, enriched with compounds **6**, **9**, and **10**, were combined (910 mg) and further purified by reversed-phase CC (ODS-A, 12 nm, S-150 mM) eluting with CH_3OH:H_2O (4:1) to afford **6** (215 mg), **9** (66 mg), and **10** (30 mg). Fraction F5 (1.1 g) was subjected to flash CC employing a $CHCl_3$/acetone gradient (30:1 → 5:1) to give compound **5** (27 mg). All isolated compounds were identified on the basis of the following spectroscopic data.

Compound ***1***. Obtained as a yellowish plate; mp 175–176 °C; ^{13}C NMR (125 MHz, $CDCl_3$) δ 18.2 (C-20), 18.6 (C-19), 21.8 (C-11), 26.2 (C-14, 15), 27.0 (C-16), 56.2 (C-3), 62.5 (OCH_3-7), 89.2 (C-4), 101.8 (C-5), 104.3 (C-9a), 111.9 (C-2), 112.8 (C-8a), 122.7 (C-12), 123.6 (C-17), 132.1 (C-18), 132.5 (C-13), 137.5 (C-8), 143.0 (C-7), 154.8 (C-6), 155.7 (C-5a), 156.1 (C-4a), 160.2 (C-1), 163.9 (C-3), 182.3 (C=O, C-9); EIMS *m/z* 424 $[M]^+$; HREIMS *m/z* 424.1891, (calcd for $C_{25}H_{28}O_6$, 424.1886).[18]

Compound ***2***. Obtained as a yellow solid; mp 155–157 °C; ^{13}C NMR (125 MHz, $CDCl_3$) δ 18.6 (C-18), 26.2 (C-19), 27.0 (C-15), 28.7 (C-13, 14), 62.5 (OCH_3-7), 78.3 (C-12), 94.6 (C-4), 102.0 (C-5),

104.2 (C-9a), 104.9 (C-2), 112.6 (C-8a), 116.1 (C-10), 123.5 (C-16), 127.6 (C-11), 132.6 (C-17), 137.4 (C-8), 143.0 (C-7), 154.9 (C-4a), 156.2 (C-5a), 156.7 (C-6), 158.3 (C-1), 160.3 (C-3), 182.4 (C=O, C-9); EIMS *m/z* 408 $[M]^+$; HREIMS *m/z* 408.1573, (calcd for $C_{24}H_{24}O_6$, 408.1573).[19]

Compound ***3***. Obtained as a yellowish powder; mp 164–166 °C; $[\alpha]_D^{28}$ +16.1 (*c* 1.0, MeOH); ^{13}C NMR (125 MHz, $CDCl_3$) δ 18.6 (C-19), 24.2 (C-15), 26.2 (C-14), 26.3 (C-20), 26.9 (C-16), 27.3 (C-11), 62.4 (OCH_3-7), 72.5 (C-13), 88.7 (C-4), 92.2 (C-12), 102.0 (C-5), 104.5 (C-2), 108.0 (C-9a), 112.5 (C-8a), 123.6 (C-17), 132.5 (C-18), 137.3 (C-18), 143.1 (C-7), 155.0 (C-6), 156.1 (C-5a), 157.5 (C-4a), 158.4 (C-1), 166.6 (C-3), 182.5 (C=O, C-9); EIMS *m/z* 426 $[M]^+$; HREIMS *m/z* 426.1682, (calcd for $C_{24}H_{26}O_7$, 426.1679).[18]

Compound ***4***. Obtained as a yellowish needle; mp 180–182 °C; ^{13}C NMR (125 MHz, acetone-d_6) δ 18.3 (C-14), 18.7 (C-19), 22.4 (C-11), 26.3 (C-20), 26.3 (C-15), 27.3 (C-16), 61.8 (OCH_3-7), 93.5 (C-4), 103.1 (C-5), 104.0 (C-9a), 111.4 (C-2), 112.4 (C-8a), 123.8 (C-12), 125.2 (C-17), 131.8 (C-13, 18), 138.5 (C-8), 144.9 (C-7), 156.1 (C-4a), 156.6 (C-6), 157.8 (C-5a), 162.1 (C-1), 163.3 (C-3), 183.2 (C=O, C-9); EIMS *m/z* 410 $[M]^+$; HREIMS *m/z* 410.1727, (calcd for $C_{24}H_{26}O_6$, 410.1729).[20]

Compound ***5***. Obtained as yellowish needles; mp 202–204 °C; ^{13}C NMR (125 MHz, acetone-d_6) δ 18.3 (C-15), 22.4 (C-11), 23.8 (C-16), 26.3 (C-14), 31.5 (C-19, 20), 46.0 (C-17), 62.1 (OCH_3-7), 71.2 (C-18), 93.6 (C-4), 103.0 (C-5), 104.0 (C-9a), 111.4 (C-2), 112.4 (C-8a), 123.9 (C-12), 131.7 (C-13), 140.4 (C-8), 144.8 (C-7), 156.1 (C-4a), 156.7 (C-5a), 157.8 (C-6), 162.1 (C-3), 163.4 (C-1), 183.2 (C=O, C-9); EIMS *m/z* 428 $[M]^+$; HREIMS *m/z* 428.1834, (calcd for $C_{24}H_{28}O_7$, 428.1835).[21]

Compound ***6***. Obtained as a yellowish crystal; mp 206–208 °C; ^{13}C NMR (125 MHz, acetone-d_6) δ 18.4 (C-14), 18.8 (C-19), 22.4 (C-11), 26.4 (C-15), 26.5 (C-20), 26.8 (C-16), 93.4 (C-4), 101.5 (C-5), 104.2 (C-9a), 111.1 (C-8a), 112.6 (C-2), 124.1 (C-12), 125.0 (C-17), 129.5 (C-8), 131.6 (C-18), 131.7 (C-13), 141.9 (C-7), 152.5 (C-5a), 153.9 (C-6), 156.1 (C-4a), 161.7 (C-1), 163.0 (C-3), 183.6 (C=O, C-9); EIMS *m/z* 396 $[M]^+$; HREIMS *m/z* 396.1574, (calcd for $C_{23}H_{24}O_6$, 396.1573).[22]

Compound ***7***. Obtained as a yellowish solid; mp 242–244 °C; ^{13}C NMR (125 MHz, DMSO-d_6) δ 18.0 (C-14), 21.3 (C-11), 25.8 (C-15), 56.8 (3-OCH_3), 90.9 (C-4), 103.2 (C-9a), 111.0 (C-2), 114.9 (C-8), 120.8 (C-6), 121.3 (C-8a), 122.2 (C-12), 124.5 (C-7), 131.4 (C-13), 145.3 (C-5a), 146.7 (C-5), 156.0 (C-4a), 158.9 (C-1), 164.5 (C-3), 180.0 (C-9); EIMS *m/z* 326 $[M]^+$; HREIMS *m/z* 326.1151, (calcd for $C_{19}H_{18}O_5$, 326.1154).[23]

Compound ***8***. Obtained as a yellowish solid; mp 165–167 °C; ^{13}C NMR (125 MHz, $CDCl_3$) δ 18.3 (C-14, 15), 22.1 (C-16), 22.5 (C-11), 26.0 (C-19), 26.2 (C-20), 103.7 (C-9a), 105.8 (C-2), 109.5 (C-4), 117.3 (C-8), 120.1 (C-6), 121.3 (C-8a), 121.6 (C-11), 122.6 (C-16), 124.2 (C-7), 133.9 (C-18), 136.6 (C-13), 144.7 (C-5a), 144.8 (C-5), 152.8 (C-4a), 159.1 (C-1), 161.3 (C-3), 181.5 (C=O, C-9); EIMS *m/z* 380 $[M]^+$; HREIMS *m/z* 380.1623, (calcd for $C_{23}H_{24}O_5$, 380.1624).[24]

Compound ***9***. Obtained as yellowish needles; mp 166–168 °C; ^{13}C NMR (125 MHz, $CDCl_3$) δ 18.3 (C-14, 19), 22.0 (C-16), 22.4 (C-11), 26.0 (C-20), 26.2 (C-15), 102.6 (C-9a), 106.2 (C-4), 107.6 (C-8a), 109.9 (C-2), 110.2 (C-7), 121.4 (C-12), 122.2 (C-17), 123.2 (C-6), 134.3 (C-18), 136.1 (C-5), 136.6 (C-13), 143.2 (C-5a), 152.9 (C-4a), 154.3 (C-8), 158.6 (C-1), 162.0 (C-3), 185.1 (C=O, C-9); EIMS *m/z* 396 $[M]^+$; HREIMS *m/z* 396.1574, (calcd for $C_{23}H_{24}O_6$, 396.1573).[25]

Compound ***10***. Obtained as a yellowish solid; mp 216–218 °C; ^{13}C NMR (125 MHz, acetone-d_6) δ 16.6 (C-14), 18.1 (C-20), 22.3 (C-11), 26.2 (C-14), 27.8 (C-16), 40.9 (C-15), 95.0 (C-4), 102.9 (C-9a), 108.8 (C-8a), 110.5 (C-7), 112.3 (C-2), 123.3 (C-12), 124.7 (C-6), 125.5 (C-2), 132.0 (C-18), 136.0 (C-13), 138.4 (C-5), 144.9 (C-5a), 154.3 (C-8), 157.0 (C-4a), 161.0 (C-3), 165.4 (C-1), 185.9 (C=O, C-9); EIMS *m/z* 396 $[M]^+$; HREIMS *m/z* 396.1576, (calcd for $C_{23}H_{24}O_6$, 396.1573).[26]

Compound ***11***. Obtained as a yellowish powder; mp 61–62 °C; $[\alpha]_D^{20}$ +1.3 (*c* 0.35, MeOH); IR, ν (KBr) cm^{-1} 3421, 2923, 2854, 1613, 1462, 1286; UV, λ_{max} nm 202, 243, 318 (MeOH); ^1H NMR (500 MHz, acetone-d_6) δ 1.52 (3H, s, H-20), 1.69 (3H, s, H-15), 1.70 (3H, s, H-19), 2.75 (1H, dd, *J* = 14.5, 8.05 Hz, H-11a), 2.94 (1H, dd, *J* = 14.5, 3.35 Hz, H-11b), 3.66 (3H, s, OCH_3-7), 3.98 (2H, d, *J* = 6.5 Hz, H-16), 4.28 (1H, m, H-12), 4.64 (1H, br s, H-14a), 4.82 (1H, br s, H-14b), 5.13 (1H, m, H-17), 6.18 (1H, s, H-4), 6.68 (1H, s, H-5) 13.9 (1H, s, 1-OH). ^{13}C NMR (125 MHz, acetone-d_6) δ 18.7 (C-15, 19), 26.3 (C-20), 27.3 (C-16), 30.5 (C-11), 61.7 (7-OCH_3), 77.1 (C-12), 94.7 (C-4), 103.2 (C-5), 103.9 (C-9a), 109.4 (C-2), 110.8 (C-14), 112.2 (C-8a), 125.2 (C-17), 131.8 (C-8), 138.5 (C-18), 145.0 (C-7), 148.7 (C-13), 156.7 (C-6), 156.7 (C-4a), 157.9 (C-5a), 162.6 (C-1), 165.1 (C-3), 183.3 (C=O, C-9); EIMS *m/z* 408 $[M]^+$; HREIMS *m/z* 408.1571 (calcd for $C_{24}H_{24}O_6$, 408.1573).

Compound ***12***. Obtained as a yellowish solid; mp 81–82 °C; $[\alpha]_D^{20}$ +11.0 (*c* 0.5, MeOH); IR, ν (KBr) cm^{-1} 3441, 2925, 2856, 1613, 1462, 1285; UV, λ_{max} nm 201, 245, 318 (MeOH); ^1H NMR (500 MHz, acetone-d_6) δ 1.51 (3H, s, H-15), 1.65 (3H, s, H-14), 1.84 (3H, s, H-20), 2.93 (1H, m, H-16b), 3.21 (2H, d, *J* = 7.2 Hz, H-11), 4.11 (1H, d, *J* = 11.5 Hz, H-16a), 4.40 (1H, d, *J* = 9.8 Hz, H-17), 4.75 (1H, s, H-19b), 5.03 (1H, s, H-19a), 5.15 (1H, br t, *J* = 14.3, 6.9 Hz, H-12), 6.28 (1H, s, H-4), 6.68 (1H, s, H-5). 13.6 (1H, s, 1-OH). ^{13}C NMR (125 MHz, acetone-d_6) δ 18.3 (C-15), 19.1 (C-20), 22.3 (C-11), 26.3 (C-14), 34.8 (C-16), 78.8 (C-17), 93.5 (C-4), 102.5 (C-5), 104.1 (C-9a), 110.6 (C-19), 111.3 (C-2), 112.4 (C-8a), 123.9 (C-12), 128.1 (C-8), 131.8 (C-13), 143.3 (C-7), 149.5 (C-18), 154.6 (C-5a), 156.3 (C-4a), 161.6 (C-6), 162.0 (C-1), 163.3 (C-3), 183.7 (C=O, C-9); EIMS *m/z* 394 $[M]^+$; HREIMS *m/z* 394.1419, (calcd for $C_{23}H_{22}O_6$, 394.1416).

4.3. Assay of neuraminidase activity

Neuraminidase activity was measured by a modification of the method described by Potier et al.[16,27] 4-Methylumbelliferyl-α-D-*N*-acetylneuraminic acid sodium salt hydrate (Sigma, M8639) 0.125 mM in 50 mM sodium acetate buffer (pH 5.0) was used as a substrate. Neuraminidase (EC 3.2.1.18. from *C. perfringens*, SIGMA, N2876) 0.02 U/mL in acetate buffer was used as the enzyme. The isolated compounds were dissolved in MeOH and diluted to the corresponding concentrations in acetate buffer. For the assay, neuraminidase (15 μL) was added to 100 μL of sample solution mixed with buffer (1635 μL) in a cuvette, and then 250 μL of substrate was added at 37 °C. 4-Methylumbelliferone was immediately quantified fluorometrically on a SpectraMax M2 Multi-Mode Microplate Reader (Molecular Devices, CA, USA). The excitation wavelength was 365 nm, and the emission wavelength was 450 nm. The determination of enzyme activity (by fitting experimental data to the logistic curve by Eq. 1), involved recording initial velocity over a range of concentrations and the data were analyzed using a nonlinear regression program [Sigma Plot (SPCC Inc., Chicago, IL)].

$$\text{Activity } (\%) = 100[1/(1 + ([I]/IC_{50}))] \quad (1)$$

4.4. Progress curves determination and time-dependent assay

Time-dependent assays and progress curves were carried out using 0.02 U/mL units neuraminidase, and 4-methylumbelliferyl-α-D-*N*-acetylneuraminic acid sodium salt hydrate (Sigma, M8639) as a substrates in 50 mM sodium acetate buffer (pH 5.0) at 37 °C. Enzyme activities were measured continuously for 5 min by fluorimetry. To determine the kinetic parameters associated with time dependent inhibition of neuraminidase, progress curves for 300 s

were obtained at several inhibitor concentrations using fixed substrate concentrations. The data were analyzed using the a nonlinear regression program [Sigma Plot (SPCC Inc., Chicago, IL)] to give the individual parameters for each curve; v_i (initial velocity), v_s (steady-state velocity), k_{obs} (apparent first-order rate constant for the transition from v_i to v_s), I (intensity at ex: 365 nm, em: 450 nm), and K_i^{app} (apparent K_i) according to the following equations:[28]

$$I = v_s t + (v_i - v_s)(1-\gamma)/k_{obs}\gamma \ln\{[1-\gamma\exp(-k_{obs}t)]/1-\gamma\} \quad (2)$$

$$v/v_0 = \exp(-k_{obs}t) \quad (3)$$

$$k_{obs} = k_6 + [(k_5 \times [I])/(K_i^{app} + [I])] \quad (4)$$

$$k_{obs} = k_4(1 + [I]/K_i^{app}) \quad (5)$$

$$K_i = k_4/k_3 \quad (6)$$

Acknowledgments

This research was supported by a grant from Technology Development Program for Agriculture and Forestry, Ministry of Agriculture and Forestry (No. 308025-05-2-HD110). H.W.R. and were supported by a scholarship from the BK21 program.

Supplementary data

Supplementary data associated with this article can be found, in the online version, at doi:10.1016/j.bmc.2010.07.033.

References and notes

1. Schauer, R.; Kelm, S.; Reuter, G.; Roggenin, P. In *Biology of the Sialic Acid*; Rosenberg, A., Ed.; Plenum Press: New York, 1995; pp 7–67.
2. Saito, M.; Yu, R. K. In *Biology of the Sialic Acid*; Rosenberg, A., Ed.; Plenum Press: New York, 1995; pp 216–313.
3. Matrosovich, M. N.; Matrosovich, T. Y.; Gray, T.; Roberts, N. A.; Klenk, H. D. *Proc. Natl. Acad. Sci. U.S.A.* **2004**, *101*, 4620.
4. Shinya, K.; Ebina, M.; Yamada, S.; Ono, M.; Kasai, N.; Kawaoka, Y. *Nature* **2006**, *440*, 435.
5. Couceiro, J. N.; Paulson, J. C.; Baum, L. G. *Virus Res.* **1993**, *29*, 155.
6. Schauer, R. *Glycoconjugate J.* **2000**, *17*, 485.
7. Varki, A. *Glycobiology* **1993**, *3*, 97.
8. Soong, G.; Muir, A.; Gomez, M. I.; Waks, J.; Reddy, B.; Planet, P.; Singh, P. K.; Kanetko, Y.; Wolfgang, M. C.; Hsiao, Y. S.; Tong, L.; Prince, A. *J. Clin. Invest.* **2006**, *116*, 2297.
9. Steenbergen, S. M.; Lichtensteiger, C. A.; Caughlan, R.; Garfinkle, J.; Fuller, T. E.; Vimr, E. R. *Infect. Immun.* **2005**, *73*, 1284.
10. Krivan, H. C.; Roberts, D. D.; Ginsburg, V. *Proc. Natl. Acad. Sci. U.S.A.* **1988**, *85*, 6157.
11. Vimr, E. R.; Kalivoda, K. A.; Deszo, E. L.; Steenbergen, S. M. *Microbiol. Mol. Biol. Rev.* **2004**, *68*, 132.
12. Chang, D. E.; Smalley, D. J.; Tucker, D. L.; Leatham, M. P.; Norris, W. E.; Stevenson, S. J.; Anderson, A. B.; Grissom, J. E.; Laux, D. C.; Cohen, P. S. *Proc. Natl. Acad. Sci. U.S.A.* **2004**, *101*, 7427.
13. Boraston, A. B.; Blean, E. F.; Healey, M. *Biochemistry* **2007**, *46*, 11352.
14. Van Immerseel, F.; De Buck, J.; Pasmans, F.; Huyghebaert, G.; Haesebrouck, F.; Ducatelle, R. *Avian Pathol.* **2004**, *33*, 537.
15. Moreno, S. A.; Boyd, E. F. *BMC Evol. Biol.* **2009**, *9*, 118.
16. Ryu, Y. B.; Curtis-Long, M. J.; Lee, J. W.; Kim, J. H.; Kim, J. Y.; Kang, K. Y.; Lee, W. S.; Park, K. H. *Bioorg. Med. Chem.* **2009**, *17*, 2744.
17. Yu, L.; Zhao, M.; Yang, B.; Zhao, Q.; Jiang, Y. *Food Chem.* **2007**, *104*, 176.
18. Suksamrarn, S.; Suwannapoch, N.; Ratananukul, P.; Aroonrerk, N.; Suksamrarn, A. *J. Nat. Prod.* **2002**, *65*, 761.
19. Suksamrarn, S.; Suwannapoch, N.; Phakhodee, W.; Thanuhiranlert, J.; Ratananukul, P.; Chimnoi, N.; Suksamrarn, A. *Chem. Pharm. Bull.* **2003**, *51*, 857.
20. Sen, A. K.; Sarkar, K. K.; Mazumder, P. C.; Banerji, N.; Uusvuori, R.; Hase, T. A. *Phytochemistry* **1982**, *21*, 1747.
21. Bennett, G. J.; Harrison, L. J.; Sia, G. L.; Sim, K. Y. *Phytochemistry* **1993**, *32*, 1245.
22. Sakai, S.-I.; Katsura, M.; Takayama, H.; Aimi, N.; Chokethaworn, N.; Suttajit, M. *Chem. Pharm. Bull.* **1993**, *41*, 958.
23. Ito, C.; Miyamoto, Y.; Rao, K. S.; Furukawa, H. *Chem. Pharm. Bull.* **1996**, *44*, 441.
24. Nguyen, L.-H. D.; Vo, H. T.; Pham, H. G.; Connolly, J. D.; Harrison, L. J. *Phytochemistry* **2003**, *63*, 467.
25. Bennett, G. J.; Lee, H. H.; Lee, L. P. *J. Nat. Prod.* **1990**, *53*, 1463.
26. Komguem, J.; Meli, A. L.; Manfouo, R. N.; Lontsi, D.; Ngounou, F. N.; Kuete, V.; Kamdem, H. W.; Tane, P.; Ngadjui, B. T.; Sondengam, B. L.; Connolly, J. D. *Phytochemistry* **2005**, *66*, 1713.
27. Potier, M.; Mameli, L.; Belisle, M.; Dallaire, L.; Melancon, S. B. *Anal. Biochem.* **1979**, *94*, 287.
28. Morrison, J. F.; Walsh, C. T. *Adv. Enzymol.* **1988**, *61*, 201.